Direct Dynamics of Gough–Stewart Hexapod Platforms Using the Redundant Parameterisation of Rotations by Full Rotation Matrices

Dan N. Dumitriu[1(✉)], Mihai Mărgăritescu[2], and Ana Maria Eulampia Rolea[2]

[1] Institute of Solid Mechanics of the Romanian Academy, 15 Constantin Mille Street, 10141 Bucharest, Romania
dumitri04@yahoo.com, dumitriu@imsar.bu.edu.ro
[2] National Institute of Research and Development for Mechatronics and Measurement Technique – INCDMTM, Şos. Pantelimon 6-8, District 2, Bucharest, Romania
mihai.margaritescu@gmail.com, eulampia46@yahoo.com

Abstract. The direct dynamics study of Gough–Stewart hexapod platforms presented in this paper represents a preparatory step towards the direct dynamics study of a double hexapod, i.e., two Gough–Stewart platforms mounted in parallel one above the other. The direct dynamics model used here is based on the redundant parameterisation of rotations by full 3×3 rotation matrices. The dynamics of each solid of the hexapod platform comprises 12 scalar differential Eqs. (3 for each translation and 9 for each solid rotation) and 6 algebraic scalar orthogonality equations, plus the algebraic constraints characterizing the joints. For the entire hexapod, the overall differential-algebraic system comprises 156 scalar differential equations and 78 + 72 = 150 scalar algebraic equations. Of course, a number of 150 scalar Lagrange multipliers are introduced in association with fulfilling the algebraic equations. So, our dynamic modelling technique involves an increased number of parameters and equations, but this disadvantage is compensated by the fact that the dynamic equations can be written in a systematic way, being structurally similar for each solid of the hexapod multibody system. From the numerical point of view, the differential-algebraic system is solved by an iterative "shooting method", using classical adaptive stepsize Runge–Kutta integration. No convergence troubles were encountered so far, when studying the direct dynamics of the Gough–Stewart hexapod platform considered as case study.

Keywords: Gough–Stewart · Hexapod platform · Direct dynamics · Redundant rotation parameterisation · Lagrange multipliers

1 Introduction

Having as project objective the control of a double hexapod platform, involving inverse kinematics but also inverse dynamics (for a good/improved force balance between leg actuators), a necessary preparatory step is the direct dynamics study of a single

G.I. Gheorghe (ed.), *Proceedings of the International Conference of Mechatronics and Cyber-MixMechatronics - 2017*, Lecture Notes in Networks and Systems 20,
DOI 10.1007/978-3-319-63091-5_7

hexapod platform. The dynamics and control of Gough–Stewart platforms (single hexapod platforms) has been intensively studied in the last two decades (e.g., see [1–4]), using Newton-Euler approach [1, 4], the Lagrange formulation [2] or the virtual work method [3], etc. These parallel robots dynamics studies use various rotation parameterisations, e.g., the Euler angles are still very popular to parameterise 3D rotations [1–3], sometimes in the framework of Denavit–Hartenberg convention.

The difference and originality of our approach consists in applying the Lagrange formulation for the redundant parameterisation of 3D rotations using rotation matrices elements (full 3×3 matrices). This choice of 9 redundant parameters for 3 rotational degrees of freedom is currently rarely used in rigid multibody dynamics, due to the fact that the redundancy means an increased number of parameters and equations, more precisely $9 - 3 = 6$ constraint equations per solid must be considered. Of course, specific Lagrange multipliers must be introduced in order to take into account these rigidity/orthogonality constraints. Other Lagrange multipliers must be considered to take into account the constraints characterizing the joints between the different solids composing the multibody system. Thus, our dynamic modelling technique involves an increased number of parameters and equations, but this disadvantage is compensated by the fact that the dynamics equations can be written in a systematic way, being structurally similar for each solid of any multibody system.

Prof. Claude Vallée has developed such a "rotationless formulation" [5], which represents a 3D rotation in rigid multibody dynamics by preserving all 9 elements of the rotation matrix and by imposing the orthogonality constraints. He focussed the research of several of his PhD students at the University of Poitiers in France on working on this "rotationless formulation", more precisely: F. Isnard contributed to consolidate and validate this "rotationless formulation", proposing the shooting method and a Lagrange multipliers elimination method as numerical solving possibilities and applying the proposed formulation to virtual reality realistic simulations [6]; Vallée and Dumitriu exploited the algebraic simplicity of the "rotationless formulation" and found new integrals of motion for a rigid body rotating about its centre of mass [7, 8]; finally, Atchonouglo et al. [9] and Monnet et al. [10] applied this redundant parameterisation method for a more precise identification of mechanical parameters, more precisely to the identification of kinematic and body segment inertial parameters in biomechanics.

The idea of using the "rotationless formulation" of SO(3) is not widely spread in mechanics, nevertheless it is not new and several authors have preferred to use this highly redundant parameterisation. Thus, Betsch et al. have preferred the representation of 3D rotations by preserving all 9 elements of the rotation matrix as parameters, in the framework of energy-momentum consistent time-stepping schemes for finite-dimensional mechanical systems with holonomic constraints [11–13]. The method of using a discrete null space matrix was used to eliminate the discrete Lagrange multipliers [11]. The same idea of eliminating explicitly the Lagrange multipliers associated with the internal zero-strain constraints is used also by Krenk and Nielsen [14], in order to reduce the size of the differential-algebraic system to be solved.

Using the same "rotationless formulation" of SO(3) special orthogonal Lie group, Gros et al. [15] obtained similar model equations in the form of index-3 differential-algebraic equations of reduced nonlinearity. They have also proposed a projection of the resulting Lagrange equations, so as to reduce the number of states that need to be

integrated by the Nonlinear Model Predictive Control. The "rotationless formulation" is also used by Seguy [16] and Samin and Fisette [17], for modular and symbolic modelling of multibody systems.

2 Single Hexapod Model

Figure 1 shows the scheme of a classical Gough–Stewart platform (single hexapod with 6 legs). Only the first leg of the single hexapod is presented in detail, being composed of its lower part S_1 and its upper part S_2. In what concerns the numbering of the solids, the second leg will be composed by its lower part S_3 and its upper part S_4 and so on. Thus, the generic notation will be as follows: S_{2i-1} (i = 1,…,6) will denote the lower parts of the six legs, being articulated to the ground/fixed base in points A_1, A_2,… and A_6, by means of cardanic/universal joints, while S_{2i} (i = 1,…,6) will denote the upper parts of the six legs, being linked to the corresponding lower part of each leg by cylindrical joints and to the end-effector platform in points B_1, B_2,… and B_6 by means of cardanic/universal joints. The end-effector platform of the single hexapod is denoted by S_{13}. The cylindrical joints allow simultaneously the translation along $\overrightarrow{A_iB_i}$ axis (i = 1,…,6) and the rotation around the same axis between the lower and the upper leg parts.

In our formulation, everything is expressed with respect to the orthonormal inertial reference frame $(O;\vec{x}_0;\vec{y}_0;\vec{z}_0)$ shown also in Fig. 1, having its origin in O which is also the centre of the irregular hexagon $A_1A_2A_3A_4A_5A_6$, placed in the fixed base plan. Axes $\vec{x}_0$ and $\vec{y}_0$ are included in this fixed basis plan $A_1A_2A_3A_4A_5A_6$, while axis $\vec{z}_0 = \vec{y}_0 \times \vec{x}_0$ is of course perpendicular. Let us denote by G_{i0} the initial position of the centre of mass G_i of solid S_i (i = 1,…,13) of the rigid multibody system.

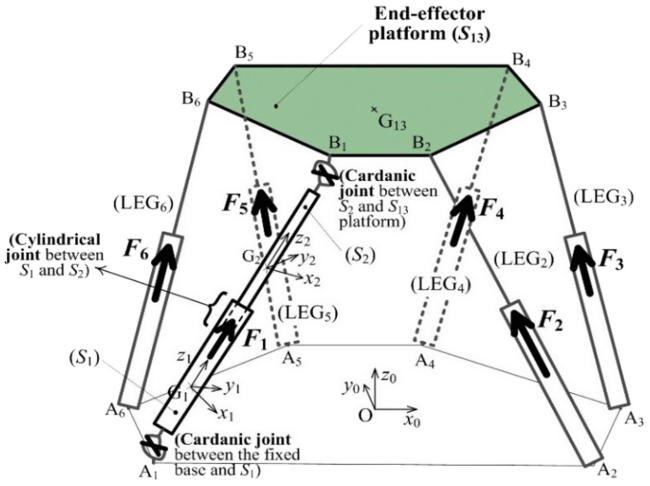

Fig. 1. Classical single hexapod model

3 Direct Dynamic Model of a Single Hexapod Using the "Rotationless Formulation"

Let us recall that "rotationless formulation" concerns the representation/parameterisation of each 3D rotation by the 9 elements of the respective 3 × 3 rotation matrix. Let us denote by $\mathbf{R}_i$ the rotation matrix of solid S_i (i = 1,…,13), while for the translation parameterisation a pseudo-translation vector $\mathbf{T}_i^*$ will be used [18], instead of the classical translation vector $\mathbf{T}_i = \overrightarrow{G_{i0}G_i}$. So, a total of 12 scalar parameters (9 for rotation and 3 for translation) will parameterise the position and motion of each solid S_i [5–10, 18]:

$$\mathbf{R}_i = \begin{bmatrix} R_{i,11} & R_{i,12} & R_{i,13} \\ R_{i,21} & R_{i,22} & R_{i,23} \\ R_{i,31} & R_{i,32} & R_{i,33} \end{bmatrix}, \text{ respectively } \mathbf{T}_i^* = \begin{bmatrix} T_{i,1}^* \\ T_{i,2}^* \\ T_{i,3}^* \end{bmatrix} = \overrightarrow{OG_i} - \mathbf{R}_i \overrightarrow{OG_{i0}} \tag{1}$$

In order to preserve the rigidity of each solid S_i, the rotation matrix $\mathbf{R}_i$ has to be an orthogonal matrix, i.e., to fulfil the rigidity/orthogonality constraint:

$$\mathbf{R}_i^{\mathrm{T}} \mathbf{R}_i = \mathbf{I}_3. \tag{2}$$

The orthogonality constraint (2) is symmetric, involving in fact only 6 scalar independent conditions to be fulfilled by the 9 elements of the 3 × 3 rotation matrix, leaving 3 = 9−6 degrees of freedom for the rotational motion of each solid S_i. So, the degree of redundancy of this parameterisation of rotations is 6.

For any point M_j of each solid S_i (i = 1,…,13) of the single hexapod, its position and velocity $\mathbf{V}(M_j)$ at any time t during the motion are given by [5–10, 18]:

$$\begin{aligned} \overrightarrow{OM_j} &= \overrightarrow{OG_i} + \overrightarrow{G_iM_j} = \overrightarrow{OG_i} + \mathbf{R}_i \overrightarrow{G_{i0}M_{j0}} = \\ &= \overrightarrow{OG_i} - \mathbf{R}_i \overrightarrow{OG_{i0}} + \mathbf{R}_i \overrightarrow{OM_{j0}} \overset{\text{definition (1)}}{=} \mathbf{T}_i^* + \mathbf{R}_i \overrightarrow{OM_{j0}}, \\ \mathbf{V}(M_j) &= \dot{\mathbf{T}}_i^* + \dot{\mathbf{R}}_i \overrightarrow{OM_{j0}}, \end{aligned} \tag{3}$$

where M_{j0} is the initial position (at time t_0 = 0) of point M_j. Definitions (3) are valid for any point M_j of each solid S_i (i = 1,…,13), showing in fact the way in which the pseudo-translation vector $\mathbf{T}_i^*$ and the rotation matrix $\mathbf{R}_i$ fully characterise the position and motion of all solids composing the rigid multibody system (single hexapod).

The derivatives of the pseudo-translation vector and of the rotation matrix are given by:

$$\begin{cases} \dot{\mathbf{R}}_i = \mathrm{j}(\boldsymbol{\Omega}_i)\, \mathbf{R}_i \\ \dot{\mathbf{T}}_i^* = \mathbf{V}(M_j) - \dot{\mathbf{R}}_i \overrightarrow{OM_{j0}} = \mathbf{V}(M_j) - \mathrm{j}(\boldsymbol{\Omega}_i)\, \mathbf{R}_i \overrightarrow{OM_{j0}} \end{cases} \tag{4}$$

where $\mathbf{\Omega}_i$ denotes the instantaneous rotation vector of solid S_i at time t, expressed in the orthonormal inertial basis $(\vec{x}_0;\vec{y}_0;\vec{z}_0)$, being defined as $\mathrm{j}(\mathbf{\Omega}_i) = \dot{\mathbf{R}}_i\mathbf{R}_i^{\mathrm{T}}$, where $\mathrm{j}(\bullet)$ is the skew-symmetric cross-product matrix defined by $\mathrm{j}(u)v = u \wedge v$, for $\forall u,v$ and with $\wedge$ denoting the classical cross-product between two 3×1 vectors.

At the initial time $t_0 = 0$, the following initial conditions in terms of the proposed redundant parameterisation must be fulfilled for each solid S_i (i = 1,…,13):

$$\begin{cases} \mathbf{R}_i(0) = \mathbf{I}_3 \\ \mathbf{T}_i^*(0) = 0 \end{cases} \quad \begin{cases} \dot{\mathbf{R}}_i(0) = \mathrm{j}(\mathbf{\Omega}_{i0}) \\ \dot{\mathbf{T}}_i^*(0) = \mathbf{V}_0(\mathrm{M}_j) - \mathrm{j}(\mathbf{\Omega}_{i0})\,\overrightarrow{\mathrm{OM}}_{j0} \end{cases} \quad (i = 1,\ldots,13) \tag{5}$$

In Lagrangian formulation, the dynamics of the rigid multibody system (our single hexapod) composed by 13 solids S_i is proved [5–10, 18] to be described by the following $12 \times 13 = 156$ Lagrange equations written in explicit form:

$$\begin{cases} \ddot{\mathbf{T}}_i^* = \dfrac{1}{m_i}\mathbf{X}_i - [(\mathbf{Y}_i + \mathbf{R}_i\mathbf{\Lambda}_i)\,\mathbf{K}_{\mathrm{G}i0}^{-1}]\,\overrightarrow{\mathrm{OG}}_{i0} \;+ \langle \mathbf{K}_{\mathrm{G}i0}^{-1}\,\overrightarrow{\mathrm{OG}}_{i0}\,,\; \overrightarrow{\mathrm{OG}}_{i0}\rangle \mathbf{X}_i \\ \ddot{\mathbf{R}}_i = (\mathbf{Y}_i + \mathbf{R}_i\mathbf{\Lambda}_i - \mathbf{X}_i \otimes \overrightarrow{\mathrm{OG}}_{i0})\mathbf{K}_{\mathrm{G}i0}^{-1}\;,\; \text{for } \forall \text{ solid } S_i\,(i = 1,\ldots,13) \end{cases} \tag{6}$$

where $\otimes$ denotes the tensor product, m_i is the mass of the solid S_i (i = 1,…,13) and G_{i0} is the initial position of the centre of mass of the solid S_i. $\mathbf{K}_{Gi0}$ is the Poinsot inertia matrix of the solid S_i calculated at the initial time in its centre of mass the point G_i, with respect to the inertial basis $(\vec{x}_0;\vec{y}_0;\vec{z}_0)$, defined by: $\mathbf{K}_{\mathrm{G}i0} = \int_{S_i} \overrightarrow{\mathrm{G}_{i0}\mathrm{M}}_{i0} \otimes \overrightarrow{\mathrm{G}_{i0}\mathrm{M}}_{i0}\,\mathrm{d}m_i$ or by its relationship with the corresponding classical inertia matrix $\mathbf{K}_{\mathrm{G}i0} = \frac{\mathrm{tr}(\mathbf{J}_{\mathrm{G}i0})}{2}\mathbf{I}_3 - \mathbf{J}_{\mathrm{G}i0}$, with the classical inertia matrix given by $\mathbf{J}_{i0} = \int_{S_i} -[\mathrm{j}\,(\overrightarrow{\mathrm{OM}}_{i0})]^2 \mathrm{d}m_i$.

Still in Eq. (6) expressing the Lagrange equations of motion for our "rotationless formulation", vector $\mathbf{X}_i$ and matrix $\mathbf{Y}_i$ are the generalized efforts acting on each solid S_i (i = 1,…,13), being composed of the external efforts acting on each solid S_i and of the internal efforts dues to the joints between S_i and other solids or between S_i and the ground. In the following, these generalized efforts will be explicitly expressed for the case of the single hexapod (Gough–Stewart platform).

$\mathbf{\Lambda}_i$ are symmetric Lagrange multipliers 3×3 matrices [5–10, 18]:

$$\mathbf{\Lambda}_i = \begin{bmatrix} \Lambda_{i,11} & \Lambda_{i,12} & \Lambda_{i,13} \\ \Lambda_{i,12} & \Lambda_{i,22} & \Lambda_{i,23} \\ \Lambda_{i,13} & \Lambda_{i,23} & \Lambda_{i,33} \end{bmatrix} \tag{7}$$

introduced in order to take into account the orthogonality condition (2) of rotation matrix $\mathbf{R}_i$. In our numerical practice, the rigidity/orthogonality constraint (2) will be considered in its double-derived form:

$$\ddot{\mathbf{R}}_i^{\mathrm{T}}\mathbf{R}_i + \mathbf{R}_i^{\mathrm{T}}\ddot{\mathbf{R}}_i + 2\,\dot{\mathbf{R}}_i^{\mathrm{T}}\dot{\mathbf{R}}_i = 0 \ \text{ for } \ \forall\, i = 1,\ldots,13. \tag{8}$$

Of course, only 6 of the 9 scalar equations of one orthogonality condition (8) are independent.

Equation (6) represent the differential part of the differential-algebraic equations governing the motion of the multibody system. Equation (6) have the same form for each solid S_i (i = 1,…,13) of the single hexapod. Of course, the inertial and geometric characteristics (m_i, $\mathbf{K}_{Gi0}$ and $\overrightarrow{OG}_{i0}$), will be different from one solid to another. But the important issue is that we have systemically/automatically the same form of these differential equations. Moreover, the differential Eqs. (6) are decoupled in what concerns their dynamic part, being linear in $\ddot{\mathbf{T}}_i^*$ and $\ddot{\mathbf{R}}_i$, which represents a major advantage from the numerical point of view.

The algebraic part of the differential-algebraic equations governing the motion of the rigid multibody system is composed by all rigidity/orthogonality constraints (8) imposing the rigidity of solids S_i, plus the constraint equations characterizing the mechanical joints between solids and with the ground. In the case of the single hexapod, there are two types of joints: cardanic/universal joints between the lower parts S_{2i-1} (i = 1,…,6) of the six legs and the ground/fixed base and between the upper parts S_{2i} (i = 1,…,6) of the six legs and the end-effector platform S_{13}, respectively the cylindrical joints in-between the lower parts and the upper parts of the six legs.

The modelling of both types of joints (cardanic/universal and cylindrical) represents an original contribution with respect to our previous work [5–10, 18]. Due to the limited length of the paper, we will not present in the following the cases of cardanic and cylindrical joints in general, but only the application of the general expressions to our single hexapod case study.

By resuming, the algebraic part of the differential-algebraic system governing the motion of the single hexapod in Fig. 1 comprises:

- the orthogonality constraints in their double-derived form (8), for $\forall\ i$ = 1,…,13;
- the algebraic equations characterizing the cardanic joints between the lower parts S_{2i-1} (i = 1,…,6) of the six legs of the single hexapod and the ground/fixed base S_0 (denoting by $A_{i,0}$ the cardanic joints centres at $t_0 = 0$, while $\mathbf{u}_{0,2i-1,0}^{\mathrm{Cardan}}$ and $\mathbf{v}_{0,2i-1,0}^{\mathrm{Cardan}}$ are the unit vectors of the two axes of the respective cardanic joint, at $t_0 = 0$):

$$\begin{cases} 0 = \mathbf{T}_{2i-1}^{*} + \mathbf{R}_{2i-1}\,\overrightarrow{OA}_{i,0} \\ \langle(-\mathbf{R}_{2i-1})\mathbf{u}_{0,2i-1,0}^{\mathrm{Cardan}},\ \mathbf{v}_{0,2i-1,0}^{\mathrm{Cardan}}\rangle = 0 \end{cases} \text{ for } \ i = 1,\ldots,6 \tag{9}$$

- the algebraic equations characterizing the cylindrical joints between the lower parts S_{2i-1} (i = 1,…,6) and the upper parts S_{2i} (i = 1,…,6) of the six legs of the single hexapod (denoting by $\mathbf{u}_{i,j,0}^{\mathrm{cyl}}$ and $\mathbf{v}_{i,j,0}^{\mathrm{cyl}}$ two distinct unit vectors perpendicular on the cylindrical joint axis at the initial time $t_0 = 0$; obviously, these two unit vectors will remain perpendicular on the cylindrical joint axis, this fact being imposed by constraints (10)):

$$\begin{cases} \langle (\mathbf{R}_{2i-1} - \mathbf{R}_{2i})\, \mathrm{A}_{i,0}\overrightarrow{\mathrm{B}}_{i,0},\ \mathbf{u}^{\mathrm{cyl}}_{2i-1,2i,0} \rangle = 0 \\ \langle (\mathbf{R}_{2i-1} - \mathbf{R}_{2i})\, \mathrm{A}_{i,0}\overrightarrow{\mathrm{B}}_{i,0},\ \mathbf{v}^{\mathrm{cyl}}_{2i-1,2i,0} \rangle = 0 \\ \langle \mathbf{R}_{2i-1}\mathbf{u}^{\mathrm{cyl}}_{2i-1,2i,0},\ \mathbf{T}^{*}_{2i} - \mathbf{T}^{*}_{2i-1} \rangle = 0 \\ \langle \mathbf{R}_{2i-1}\mathbf{v}^{\mathrm{cyl}}_{2i-1,2i,0},\ \mathbf{T}^{*}_{2i} - \mathbf{T}^{*}_{2i-1} \rangle = 0 \end{cases} \quad \text{for } i = 1, \ldots, 6 \tag{10}$$

- the algebraic equations characterizing the cardanic joints between the upper parts S_{2i} (i = 1,…,6) of the 6 legs of the single hexapod and the end-effector platform S_{13}:

$$\begin{cases} \mathbf{T}^{*}_{2i} + \mathbf{R}_{2i}\overrightarrow{\mathrm{OB}}_{i,0} = \mathbf{T}^{*}_{13} + \mathbf{R}_{13}\overrightarrow{\mathrm{OB}}_{i,0} \\ \langle (\mathbf{R}_{13} - \mathbf{R}_{2i})\mathbf{u}^{\mathrm{Cardan}}_{2i,13,0},\ \mathbf{v}^{\mathrm{Cardan}}_{2i,13,0} \rangle = 0 \end{cases} \text{ for } i = 1, \ldots, 6 \tag{11}$$

where $\mathrm{B}_{i,0}$ are the centres of these cardanic joints at the initial time $t_0 = 0$, while $\mathbf{u}^{\mathrm{Cardan}}_{2i,13,0}$ and $\mathbf{v}^{\mathrm{Cardan}}_{2i,13,0}$ are the unit vectors of the two axes of the respective cardanic joint, obviously considered also at $t_0 = 0$.

In what concerns the generalized efforts, the ones acting on the lower parts $S_{2i\text{-}1}$ (i = 1,…,6) of the six legs of the single hexapod are given by:

$$\begin{cases} \mathbf{X}_{2i-1} = \mathbf{X}^{\mathrm{ext}}_{2i-1} + \mathbf{X}^{\mathrm{Cardan}}_{2i-1\leftarrow 0} + \mathbf{X}^{\mathrm{cyl}}_{2i-1\leftarrow 2i} = -m_{i,\mathrm{inf}}\, g\, \vec{\mathbf{z}}_0 - \boldsymbol{\Lambda}^{\mathrm{Cardan}}_{0,2i-1} - \mathbf{R}_{2i-1}(\lambda^{\mathrm{cyl}}_{2i-1,2i,u2}\mathbf{u}^{\mathrm{cyl}}_{2i-1,2i,0} + \lambda^{\mathrm{cyl}}_{2i-1,2i,v2}\mathbf{v}^{\mathrm{cyl}}_{2i-1,2i,0}) \\ \mathbf{Y}_{2i-1} = \mathbf{Y}^{\mathrm{ext}}_{2i-1} + \mathbf{Y}^{\mathrm{Cardan}}_{2i-1\leftarrow 0} + \mathbf{Y}^{\mathrm{cyl}}_{2i-1\leftarrow 2i} = -m_{i,\mathrm{inf}}\, g\, \vec{\mathbf{z}}_0 \otimes \overrightarrow{\mathrm{OG}}_{2i-1,0} - \boldsymbol{\Lambda}^{\mathrm{Cardan}}_{0,2i-1} \otimes \overrightarrow{\mathrm{OA}}_{i,0} - \\ \quad -\lambda^{\mathrm{Cardan}}_{0,2i-1,u}(\mathbf{v}^{\mathrm{Cardan}}_{0,2i-1,0} \otimes \mathbf{u}^{\mathrm{Cardan}}_{0,2i-1,0}) + (\lambda^{\mathrm{cyl}}_{2i-1,2i,u}\mathbf{u}^{\mathrm{cyl}}_{2i-1,2i,0} + \lambda^{\mathrm{cyl}}_{2i-1,2i,v}\mathbf{v}^{\mathrm{cyl}}_{2i-1,2i,0}) \otimes \mathrm{A}_{i,0}\overrightarrow{\mathrm{B}}_{i,0} \\ \qquad + (\mathbf{T}^{*}_{2i} - \mathbf{T}^{*}_{2i-1}) \otimes (\lambda^{\mathrm{cyl}}_{2i-1,2i,u2}\mathbf{u}^{\mathrm{cyl}}_{2i-1,2i,0} + \lambda^{\mathrm{cyl}}_{2i-1,2i,v2}\mathbf{v}^{\mathrm{cyl}}_{2i-1,2i,0}),\ \forall i = 1, \ldots, 6 \end{cases} \tag{12}$$

The generalized efforts acting on the upper parts S_{2i} (i = 1,…,6) of the six legs of the single hexapod are:

$$\begin{cases} \mathbf{X}_{2i} = \mathbf{X}^{\mathrm{ext}}_{2i} + \mathbf{X}^{\mathrm{cyl}}_{2i\leftarrow 2i-1} + \mathbf{X}^{\mathrm{Cardan}}_{2i\leftarrow 13} = F_i\, \vec{\mathbf{z}}_i - m_{i,\mathrm{sup}} g\, \vec{\mathbf{z}}_0 + \mathbf{R}_{2i-1}(\lambda^{\mathrm{cyl}}_{2i-1,2i,u2}\mathbf{u}^{\mathrm{cyl}}_{2i-1,2i,0} + \lambda^{\mathrm{cyl}}_{2i-1,2i,v2}\mathbf{v}^{\mathrm{cyl}}_{2i-1,2i,0}) + \boldsymbol{\Lambda}^{\mathrm{Cardan}}_{2i,13} \\ \mathbf{Y}_{2i} = \mathbf{Y}^{\mathrm{ext}}_{2i} + \mathbf{Y}^{\mathrm{cyl}}_{2i\leftarrow 2i-1} + \mathbf{Y}^{\mathrm{Cardan}}_{2i\leftarrow 13} = F_i\, \vec{\mathbf{z}}_i \otimes \overrightarrow{\mathrm{OP}}_{F_i,\,0} - m_{i,\mathrm{sup}} g\, \vec{\mathbf{z}}_0 \otimes \overrightarrow{\mathrm{OG}}_{2i,0} + \boldsymbol{\Lambda}^{\mathrm{Cardan}}_{2i,13} \otimes \overrightarrow{\mathrm{OB}}_{i,0} + \\ \qquad + \lambda^{\mathrm{Cardan}}_{2i,13,u}(\mathbf{v}^{\mathrm{Cardan}}_{2i,13,0} \otimes \mathbf{u}^{\mathrm{Cardan}}_{2i,13,0}) - (\lambda^{\mathrm{cyl}}_{2i-1,2i,u}\mathbf{u}^{\mathrm{cyl}}_{2i-1,2i,0} + \lambda^{\mathrm{cyl}}_{2i-1,2i,v}\mathbf{v}^{\mathrm{cyl}}_{2i-1,2i,0}) \otimes \mathrm{A}_{i,0}\overrightarrow{\mathrm{B}}_{i,0} \\ \qquad -(\mathbf{T}^{*}_{2i} - \mathbf{T}^{*}_{2i-1}) \otimes (\lambda^{\mathrm{cyl}}_{2i-1,2i,u2}\mathbf{u}^{\mathrm{cyl}}_{2i-1,2i,0} + \lambda^{\mathrm{cyl}}_{2i-1,2i,v2}\mathbf{v}^{\mathrm{cyl}}_{2i-1,2i,0}),\ \forall i = 1, \ldots, 6 \end{cases} \tag{13}$$

Finally, the end-effector platform S_{13} is actuated by the following generalized efforts $\mathbf{X}_{13}$ and $\mathbf{Y}_{13}$:

$$\begin{cases} \mathbf{X}_{13} = \mathbf{X}^{\mathrm{ext}}_{13} + \sum_{i=1}^{6} \mathbf{X}^{\mathrm{Cardan}}_{13\leftarrow 2i} = -m_{13} g\, \vec{\mathbf{z}}_0 - \sum_{i=1}^{6} \boldsymbol{\Lambda}^{\mathrm{Cardan}}_{2i,13} \\ \mathbf{Y}_{13} = \mathbf{Y}^{\mathrm{ext}}_{13} + \sum_{i=1}^{6} \mathbf{Y}^{\mathrm{Cardan}}_{13\leftarrow 2i} = -m_{13} g\, \vec{\mathbf{z}}_0 \otimes \overrightarrow{\mathrm{OG}}_{13,0} - \sum_{i=1}^{6} \boldsymbol{\Lambda}^{\mathrm{Cardan}}_{2i,13} \otimes \overrightarrow{\mathrm{OB}}_{i,0} - \sum_{i=1}^{6} \lambda^{\mathrm{Cardan}}_{2i,13,u}(\mathbf{v}^{\mathrm{Cardan}}_{2i,13,0} \otimes \mathbf{u}^{\mathrm{Cardan}}_{2i,13,0}) \end{cases} \tag{14}$$

4 Single Hexapod Numerical Case Study

A single hexapod with 6 identical legs and with the fixed base S_0 and end-effector platform S_{13} having the form of planar irregular convex hexagons with symmetry ($A_1A_2A_3A_4A_5A_6$ and $B_1B_2B_3B_4B_5B_6$, respectively) is studied here. The following inertial and geometric characteristics are considered in this case study:

- for the lower parts of each of the 6 identical legs: mass $m_{2i\text{-}1} = m_{\text{lower}} = 0.7$ [kg]; length $l_{2i\text{-}1} = l_{\text{lower}} = 0.40$ [m]; Poinsot inertia matrix of the solid $S_{2i\text{-}1}$ ($i = 1,\ldots,6$) calculated at the initial time in its centre of mass $G_{2i\text{-}1}$, with respect to the local orthonormal basis $\left(\vec{x}_{2i-1,0}; \vec{y}_{2i-1,0}; \vec{z}_{2i-1,0}\right)$, attached to lower leg $S_{2\text{i-}1}$ (i = 1,…,6):

$$\mathbf{K}_{\text{G},2i-1} = [0,\ 0,\ 0;\ 0,\ 0,\ 0;\ 0,\ 0,\ 0.0071]\ [\text{kg} \cdot \text{m}^2];$$

- for the upper parts of each of the 6 identical legs: mass $m_{2i} = m_{\text{upper}} = 0.3$ [kg]; length $l_{2i} = l_{\text{upper}} = 0.40$ [m]; Poinsot inertia matrix of the solid S_{2i} ($i = 1,\ldots,6$) calculated at the initial time in its centre of mass G_{2i}, with respect to the local orthonormal basis $\left(\vec{x}_{2i,0}; \vec{y}_{2i,0}; \vec{z}_{2i,0}\right)$, attached to upper leg $S_{2\text{i}}$ (i = 1,…,6):

$$\mathbf{K}_{\text{G},2i} = [0,\ 0,\ 0;\ 0,\ 0,\ 0;\ 0,\ 0,\ 0.0031]\ [\text{kg} \cdot \text{m}^2];$$

- for the end-effector platform: mass $m_{13} = m_{\text{platform}} = 3$ [kg]; Poinsot inertia matrix of the end-effector platform S_{13} calculated at the initial time in its centre of mass the point G_{13}, with respect to the local orthonormal basis $(\vec{x}_{13}; \vec{y}_{13}; \vec{z}_{13})$, attached to the end-effector platform S_{13}:

$$\mathbf{K}_{\text{G},13} = \mathbf{K}_{\text{G},13,0} = [0.0324,\ 0,\ 0;\ 0,\ 0.0324,\ 0;\ 0,\ 0,\ 0]\ [\text{kg} \cdot \text{m}^2].$$

The fixed basis $A_1A_2A_3A_4A_5A_6$ is a planar irregular convex hexagon with symmetry having its circumscribed circle of circumcentre O and circumradius $r_{\text{basis},S0} = 0.40$ [m], with angles $\angle A_1OA_2 = \angle A_3OA_4 = \angle A_5OA_6 = 90°$ and $\angle A_2OA_3 = \angle A_4OA_5 = \angle A_6OA_1 = 30°$.

The end-effector platform $B_1B_2B_3B_4B_5B_6$ is a planar irregular convex hexagon with symmetry having its circumscribed circle of circumcentre G_{13} and circumradius $r_{\text{platform},S13} = 0.35$[m], with angles $\angle B1OB2 = \angle B3OB4 = \angle B5OB6 = 36°$ and $\angle B_2OB_3 = \angle B_4OB_5 = \angle B_6OB_1 = 84°$.

At the initial time $t_0 = 0$, the length of the 6 identical legs is considered the same: $l_{\text{leg-}i,0} = 0.5320$ [m] ($i = 1,\ldots,6$). For this initial configuration of the single hexapod, one computes for the first leg (similarly for the others):

$$\overrightarrow{\mathrm{OA}}_{1,0} = r_{\mathrm{basis},S_0}\sin\frac{90^\circ}{2}\,\vec{\mathbf{x}}_0 - r_{\mathrm{basis},S_0}\cos\frac{90^\circ}{2}\,\vec{\mathbf{y}}_0,\ \overrightarrow{\mathrm{OB}}_{1,0} = h_0\,\vec{\mathbf{z}}_0 + r_{\mathrm{platf.},S_{13}}\sin\frac{36^\circ}{2}\,\vec{\mathbf{x}}_0 - r_{\mathrm{platf.},S_{13}}\cos\frac{36^\circ}{2}\,\vec{\mathbf{y}}_0,$$
$$h_0 = \sqrt{l_{1,0}^2 - \left(r_{\mathrm{platform},S_{13}}\sin\frac{36^\circ}{2} - r_{\mathrm{basis},S_0}\sin\frac{90^\circ}{2}\right)^2 - \left(r_{\mathrm{platform},S_{13}}\cos\frac{36^\circ}{2} - r_{\mathrm{basis},S_0}\cos\frac{90^\circ}{2}\right)^2},$$
$$\mathrm{A}_{1,0}\overrightarrow{\mathrm{B}}_{1,0} = \overrightarrow{\mathrm{OB}}_{1,0} - \overrightarrow{\mathrm{OA}}_{1,0},\ \vec{\mathbf{z}}_1 = \vec{\mathbf{z}}_2 = \frac{\overrightarrow{\mathrm{A}_{1,0}\mathrm{B}_{1,0}}}{||\mathrm{A}_{1,0}\mathrm{B}_{1,0}||},$$
$$\overrightarrow{\mathrm{OG}}_{1,0} = \overrightarrow{\mathrm{OA}}_{1,0} + \frac{l_{\mathrm{lower},0}}{2}\vec{\mathbf{z}}_1\ (\mathrm{G}_1 \equiv \mathrm{G}_{\mathrm{leg}-1,\mathrm{lower}}),\ \overrightarrow{\mathrm{OG}}_{2,0} = \overrightarrow{\mathrm{OB}}_{1,0} - \frac{l_{\mathrm{upper}}}{2}\vec{\mathbf{z}}_1\ (\mathrm{G}_2 \equiv \mathrm{G}_{\mathrm{leg}-1,\mathrm{sup}}),$$
$$\overrightarrow{\mathrm{OP}}_{F_1,0} = \overrightarrow{\mathrm{OB}}_{1,0} - l_{\mathrm{upper}}\,\vec{\mathbf{z}}_1\ (\mathrm{P}_{F_1} \equiv \text{application point of } F_1),\ \overrightarrow{\mathrm{OG}}_{13,0} = h_0\,\vec{\mathbf{z}}_0\,. \tag{15}$$

As it can be deduced, the forces are considered to be applied on the upper parts of the legs, at their lower extremity. To statically support the end-effector platform in its initial position, the numerical code based on the direct dynamics model proposed in this paper provides the following necessary forces: $F_1 = F_2 = F_3 = F_4 = F_5 = F_6 = 8.5105$ [N]. These forces seem to coincide with the simple analytical calculations corresponding to the static equilibrium of the platform in the considered initial position.

The second validation simple dynamic test concerns the application of the following forces:

$$F_1 = F_2 = 9.5[\mathrm{N}], F_3 = F_4 = F_5 = F_6 = 8.5105[\mathrm{N}]. \tag{16}$$

Since with respect to the static equilibrium case study only forces F_1 and F_2 are slightly modified, also due to the symmetry of the single hexapod, it is logical to expect a rotation of the end-effector platform S_{13} around $\vec{x}_0$ axis (which is in fact the case, as shown in Fig. 3 only angle φ_2 presents a variation/evolution).

Figure 2 shows the evolution in time (between 0 and 0.5 s) of the classical translation vector $\mathbf{T}_{13} = \mathrm{G}_{13,0}\overrightarrow{\mathrm{G}_{13}}$ of the end-effector platform S_{13}, of course computed from $\mathbf{T}_{13}^*$ and $\mathbf{R}_{13}$ as:

$$\mathbf{T}_{13} = \mathrm{G}_{13,0}\overrightarrow{\mathrm{G}_{13}} = \overrightarrow{\mathrm{OG}_{13}} - \overrightarrow{\mathrm{OG}_{13,0}} = \mathbf{T}_{13}^* + \mathbf{R}_{13}\,\overrightarrow{\mathrm{OG}_{13,0}} - \overrightarrow{\mathrm{OG}_{13,0}} \tag{17}$$

Figure 3 shows the evolution in time of the Tait–Bryant angles (called also Cardan angles, or even x-y-z sequence of rotations), extracted from the rotation matrix $\mathbf{R}_{13}$ of the end-effector platform S_{13}, based on the following correspondence relation:

$$\mathbf{R} = \begin{bmatrix} \cos\varphi_2\cos\varphi_3 & \sin\varphi_1\sin\varphi_2\cos\varphi_3 + \cos\varphi_1\sin\varphi_3 & -\cos\varphi_1\sin\varphi_2\cos\varphi_3 + \sin\varphi_1\sin\varphi_3 \\ -\cos\varphi_2\sin\varphi_3 & -\sin\varphi_1\sin\varphi_2\sin\varphi_3 + \cos\varphi_1\cos\varphi_3 & \cos\varphi_1\sin\varphi_2\sin\varphi_3 + \sin\varphi_1\cos\varphi_3 \\ \sin\varphi_2 & -\sin\varphi_1\cos\varphi_2 & \cos\varphi_1\cos\varphi_2 \end{bmatrix} \tag{18}$$

As observed, the three Tait–Bryant angles were denoted by φ_1, φ_2 and φ_3.

Finally, Fig. 4 shows the variation in time of the lengths of the 6 legs of the single hexapod, corresponding to the motion imposed by forces (16) of the considered case study. Obviously, due to the particular symmetry of the considered case study, one has: $l_1 = l_2$, $l_5 = l_4$ and $l_6 = l_3$.

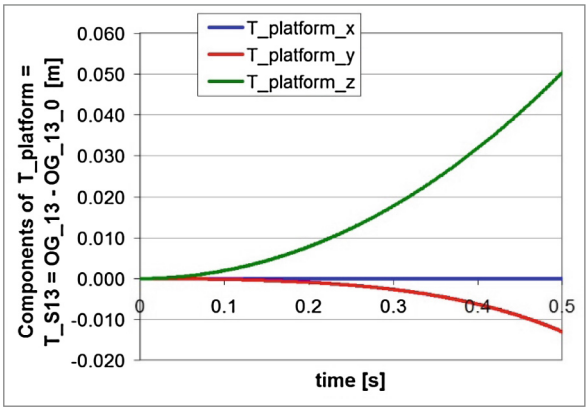

Fig. 2. Evolution in time of the classical translation vector of the end-effector platform S_{13}

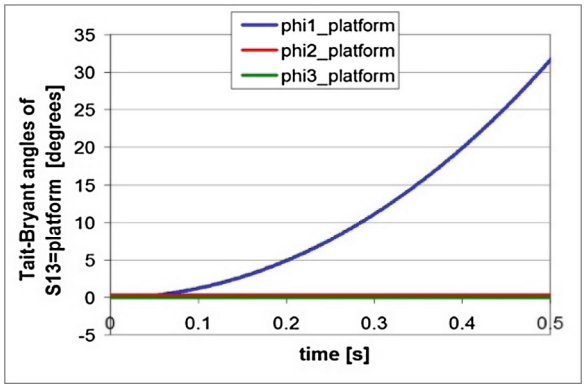

Fig. 3. Evolution in time of the Tait–Bryant angles corresponding to the rotation $\mathbf{R}_{13}$ of platform S_{13}

The results presented in Figs. 2, 3, and 4 seem normal for the considered case study. Of course, an inverse dynamics simulation would have been more suggestive, but this will be the topics of a future paper. So far, the results have been validated using an in-house LabView inverse kinematics modelling and simulation software [19]. More precisely, the correct correspondence between the platform position and orientation evolution and the variation of the lengths of the six legs has been successfully verified. Figure 5 shows the graphical user interface of this in-house LabView single hexapod inverse kinematics tool, which has already been validated on several case studies, so it can be considered as a valid virtual experiment.

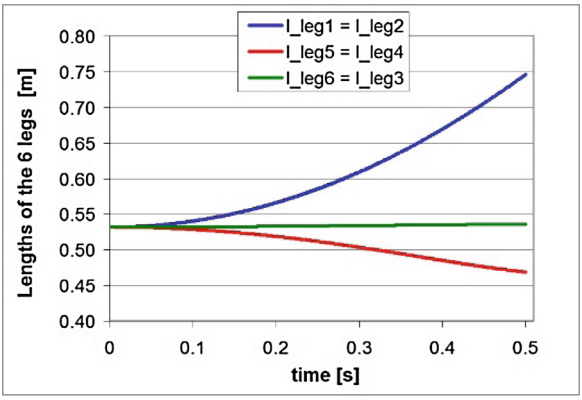

Fig. 4. Variation in time of the lengths of the six legs of the single hexapod, corresponding to the imposed motion

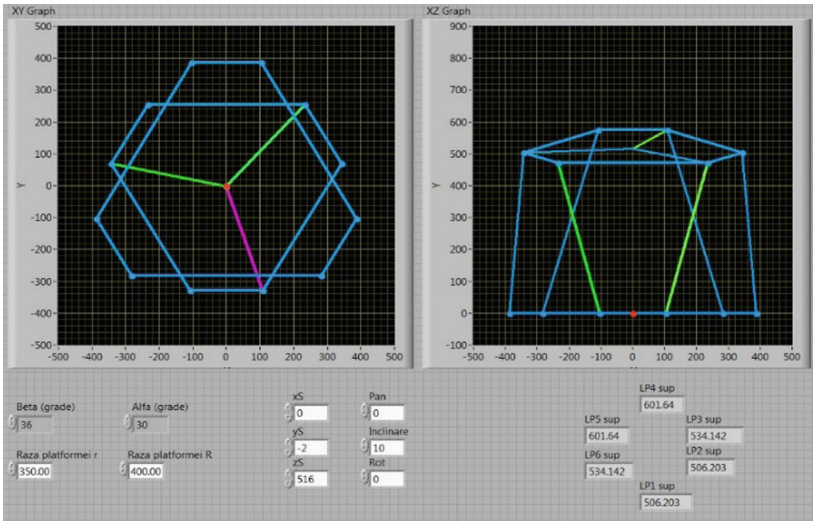

Fig. 5. LabView single hexapod inverse kinematics validation tool

5 Conclusions and Future Work

Already tested on simpler case studies [5–10, 18], the "rotationless formulation" proposed by C. Vallée et al. is applied here for a single hexapod. More precisely, the proposed redundant representation of rotations concerns the parameterisation of each 3D rotation by the 9 elements of the respective 3×3 rotation matrix. Using this 3D rotations representation in Lagrange formulation, one obtains for the single hexapod direct dynamics a differential-algebraic system composed by: 156 scalar differential

equations, plus 78 scalar rigidity/orthogonality constraints (algebraic equations) and other 72 scalar algebraic equations characterizing the joints of the rigid multibody system which is the single hexapod. The unknowns are 156 scalar elements of the pseudo-translation vectors and rotation matrices of all 13 solids of the single hexapod, plus 150 Lagrange multipliers introduced in order to take into account the algebraic constraints. In conclusion, the number of equations corresponds to the number of unknowns, thus the differential-algebraic system has been solved classically by an iterative "shooting method", with classical adaptive stepsize Runge–Kutta integration. From the numerical point of view, no convergence troubles were encountered so far, when studying the direct dynamics of the Gough–Stewart hexapod platform considered as case study.

As further work, an inverse dynamics study for the single hexapod is foreseen. On the other hand, since the project acknowledged by the authors concerns a double hexapod, obviously our future work will be extended to the direct and inverse dynamics of a double hexapod, i.e., two Gough–Stewart platforms mounted in parallel one above the other.

Acknowledgements. This work was supported by a grant of the Romanian National Authority for Scientific Research and Innovation, CNCS/CCCDI - UEFISCDI, project number PNIII-P2-2. 1-PED-2016-0412, contract nr. 50 PED/2017, within PNCDI III.

References

1. Leonov, G.A., Zegzhda, S.A., Zuev, S.M., Ershov, B.A., Kazunin, D.V., Kostygova, D.M., Kuznetsov, N.V., Tovstik, P.E., Tovstik, T.P., Yushkov, M.P.: Dynamics and control of the Stewart platform. Dokl. Phys. **59**(9), 405–410 (2014)
2. Bingul, Z., Karahan, O.: Dynamic modeling and simulation of Stewart platform. In: Küçük, S. (ed.) Serial and Parallel Robot Manipulators—Kinematics, Dynamics, Control and Optimization, pp. 19–42. INTECH Open Access Publisher, Rijeka (2012)
3. Kalani, H., Rezaei, A., Akbarzadeh, A.: Improved general solution for the dynamic modeling of Gough–Stewart platform based on principle of virtual work. Nonlinear Dyn. **83**(4), 2393–2418 (2016)
4. Pedrammehr, S., Mahboubkhah, M., Khani, N.: Improved dynamic equations for the generally configured Stewart platform manipulator. J. Mech. Sci. Technol. **26**(3), 711–721 (2012)
5. Vallée, C., Hamdouni, A., Isnard, F., Fortuné, D.: The equations of motion of a rigid body without parametrization of rotations. J. Appl. Math. Mech. **63**(1), 25–30 (1999)
6. Isnard, F., Dodds, G., Vallée, C., Fortuné, D.: Real-time dynamics simulation of a closed-chain robot within a virtual reality environment. Proc. Inst. Mech. Eng. Part K: J. Multi-body Dyn. **214**(4), 219–232 (2000)
7. Vallée, C., Dumitriu, D.: The Lagrange multipliers associated with the rotation matrix characterizing the motion of a rigid body about its centre of mass. J. Appl. Math. Mech. **65**(5), 731–739 (2001)
8. Dumitriu, D., Vallée, C.: Matricial Approach of Rigid Multibody Dynamics. BREN Publishing House, Bucharest (2011). (in Romanian)

9. Atchonouglo, K., Vallée, C., Monnet, T., Fortuné, D.: Identification of the ten inertia parameters of a rigid body. J. Appl. Math. Mech. **72**(1), 22–25 (2008)
10. Monnet, T., Begon, M., Vallée, C., Lacouture, P.: Improvement of the input data in biomechanics: kinematic and body segment inertial parameters. In: Levy, J.H. (ed.) Biomechanics: Principles, Trends and Applications, pp. 353–385. Nova Science Publishers, London (2010). Chapter 15
11. Betsch, P.: The discrete null space method for the energy consistent integration of constrained mechanical systems. Part I: holonomic constraints. Comput. Methods Appl. Mech. Eng. **194**(50–52), 5159–5190 (2005)
12. Betsch, P., Leyendecker, S.: The discrete null space method for the energy consistent integration of constrained mechanical systems. Part II: multibody dynamics. Int. J. Numer. Methods. Eng. **67**(4), 499–552 (2006)
13. Uhlar, S., Betsch, P.: A rotationless formulation of multibody dynamics: modeling of screw joints and incorporation of control constraints. Multibody Syst. Dyn. **22**(1), 69–95 (2009)
14. Krenk, S., Nielsen, M.B.: Conservative rigid body dynamics by convected base vectors with implicit constraints. Comput. Methods Appl. Mech. Eng. **269**, 437–453 (2014)
15. Gros, S., Zanon, M., Vukov, M., Diehl, M.: Nonlinear MPC and MHE for mechanical multi-body systems with application to fast tethered airplanes. In: 4th IFAC Nonlinear Model Predictive Control Conference, Noordwijkerhout, NL, 23–27 August 2012, pp. 86–93 (2012)
16. Seguy, N.: Modélisation modulaire de systèmes articulés: Conception orientée-objet de plates-formes de simulation. Ph.D. thesis (in French, advisor: Pascal, M.), University of Evry Val d'Essonne, France (2003)
17. Samin, J.-C., Fisette, P.: Symbolic Modeling of Multibody Systems. Kluwer Academic Publishers, Dordrecht (2003)
18. Dumitriu, D., Mărgăritescu, M.: Validation of new rigid body dynamics formulation using rotation matrices elements as dependent parameters–double pendulum case study. Rom. J. Tech. Sci. - Appl. Mech. **60**(3), 231–252 (2015)
19. Mărgăritescu, M., Ivan, A.M.E., Văduva, V., Brişan, C.: Extended mobility carried out with a double hexapod robot. In: Solid State Phenomena, vol. 166–167, pp. 271–276. Trans Tech Publications, Zurich (2010)